Immune cell Toll-like receptor 4 mediates the development of obesity- and endotoxemia-associated adipose tissue fibrosis.

Isabelle K Vila, Pierre-Marie Badin, Marie-Adeline Marques, Laurent Monbrun, Corinne Lefort, Lucile Mir, Katie Louche, Virginie Bourlier, Balbine Roussel, Philippe Gui, et al.

Please cite this article in press as: Vila et al., Immune Cell Toll-like Receptor 4 Mediates the Development of Obesity- and Endotoxemia-Associated Adipose Tissue Fibrosis, Cell Reports (2014), http://dx.doi.org/10.1016/j.celrep.2014.03.062

Cell Reports
Article

Immune Cell Toll-like Receptor 4 Mediates the Development of Obesity- and Endotoxemia-Associated Adipose Tissue Fibrosis

Isabelle K. Vila,[1,2,3] Pierre-Marie Badin,[1,2,3] Marie-Adeline Marques,[1,2,3] Laurent Monbrun,[1,2,3] Corinne Lefort,[1,2,3] Lucile Mir,[1,2,3] Katie Louche,[1,2,3] Virginie Bourlier,[1,2,3] Balbine Roussel,[1,2,3] Philippe Gui,[2,3] Jacques Grober,[4,5] Vladimír Štich,[6,7] Lenka Rossmeislová,[6,7] Alexia Zakaroff-Girard,[3,8] Anne Bouloumié,[3,8] Nathalie Viguerie,[1,2,3] Cedric Moro,[1,2,3] Geneviève Tavernier,[1,2,3] and Dominique Langin[1,2,3,9,*]

[1]Franco-Czech Laboratory for Clinical Research on Obesity, Inserm, 31432 Toulouse Cedex 4, France
[2]Obesity Research Laboratory, Institute of Metabolic and Cardiovascular Diseases, UMR1048, Inserm, 31432 Toulouse Cedex 4, France
[3]UMR1048, Paul Sabatier University, University of Toulouse, 31432 Toulouse Cedex 4, France
[4]UMR866, Inserm, 21000 Dijon, France
[5]LabEx lipSTIC, Faculty of Medicine, University of Burgundy, 21000 Dijon, France
[6]Franco-Czech Laboratory for Clinical Research on Obesity, Third Faculty of Medicine, 100 00 Prague 10, Czech Republic
[7]Department of Sport Medicine, Third Faculty of Medicine, Charles University, 100 00 Prague 10, Czech Republic
[8]Laboratory of Vascular Network, Immune Cells, and Progenitor Cells in the Adipose Tissue, Institute of Metabolic and Cardiovascular Diseases, UMR1048, Inserm, 31432 Toulouse Cedex 4, France
[9]Department of Clinical Biochemistry, Toulouse University Hospitals, 31059 Toulouse Cedex 9, France
*Correspondence: dominique.langin@inserm.fr
http://dx.doi.org/10.1016/j.celrep.2014.03.062

SUMMARY

Adipose tissue fibrosis development blocks adipocyte hypertrophy and favors ectopic lipid accumulation. Here, we show that adipose tissue fibrosis is associated with obesity and insulin resistance in humans and mice. Kinetic studies in C3H mice fed a high-fat diet show activation of macrophages and progression of fibrosis along with adipocyte metabolic dysfunction and death. Adipose tissue fibrosis is attenuated by macrophage depletion. Impairment of Toll-like receptor 4 signaling protects mice from obesity-induced fibrosis. The presence of a functional Toll-like receptor 4 on adipose tissue hematopoietic cells is necessary for the initiation of adipose tissue fibrosis. Continuous low-dose infusion of the Toll-like receptor 4 ligand, lipopolysaccharide, promotes adipose tissue fibrosis. Ex vivo, lipopolysaccharide-mediated induction of fibrosis is prevented by antibodies against the profibrotic factor TGFβ1. Together, these results indicate that obesity and endotoxemia favor the development of adipose tissue fibrosis, a condition associated with insulin resistance, through immune cell Toll-like receptor 4.

INTRODUCTION

Adipose tissue (AT) serves as a long-term energy reserve that can be mobilized during food deprivation. Under excess energy conditions, AT expands through storage of fatty acids as triglycerides. AT expansion protects other organs against chronic lipid overload, leading to metabolic disorders. Indeed, facilitated AT expansion is associated in transgenic mouse models with a better metabolic state (Kim et al., 2007; Kusminski et al., 2012; Medina-Gomez et al., 2007; Virtue and Vidal-Puig, 2008). Lack of AT, as seen in lipodystrophy, leads to severe metabolic abnormalities (Gandotra et al., 2011; Pajvani et al., 2005). During AT expansion in mice fed a high-fat diet (HFD), there is a remodeling of the tissue to accommodate adipocyte growth (Strissel et al., 2007). In the obese state, AT remodeling is characterized by immune cell infiltration, cytokine release, and production of extracellular matrix (ECM) (Sun et al., 2013). Mice lacking collagen VI, a type of collagen found in human and mouse AT, show increased expansion of AT and improvements in whole-body energy homeostasis (Divoux et al., 2010; Khan et al., 2009). Therefore, excessive collagen accumulation and development of fibrosis can limit AT expandability, resulting in ectopic lipid accumulation and development of metabolic syndrome.

Obesity in humans and mice is characterized by systemic and AT inflammation (Cancello et al., 2005; Klimcakova et al., 2011a; Weisberg et al., 2003; Xu et al., 2003). This state of low-grade inflammation results in increased production of cytokines and chemokines, primarily by macrophages (Horng and Hotamisligil, 2011). In liver and kidney, there is a close link between inflammation, production of ECM and development of fibrosis. In these organs, there is mounting evidence that the immune Toll-like receptor 4 (TLR4) acts as a key regulator in fibrogenesis (Aoyama et al., 2010; Campbell et al., 2011; Seki et al., 2007). A role for TLR4 in AT macrophage response has been shown, but its direct contribution to AT fibrosis remains elusive (Poggi et al., 2007; Saberi et al., 2009; Shi et al., 2006).

Despite its importance in the dynamics of AT remodeling and consequences on metabolic status, the mechanisms controlling AT fibrosis remain poorly understood. One of the limitations has

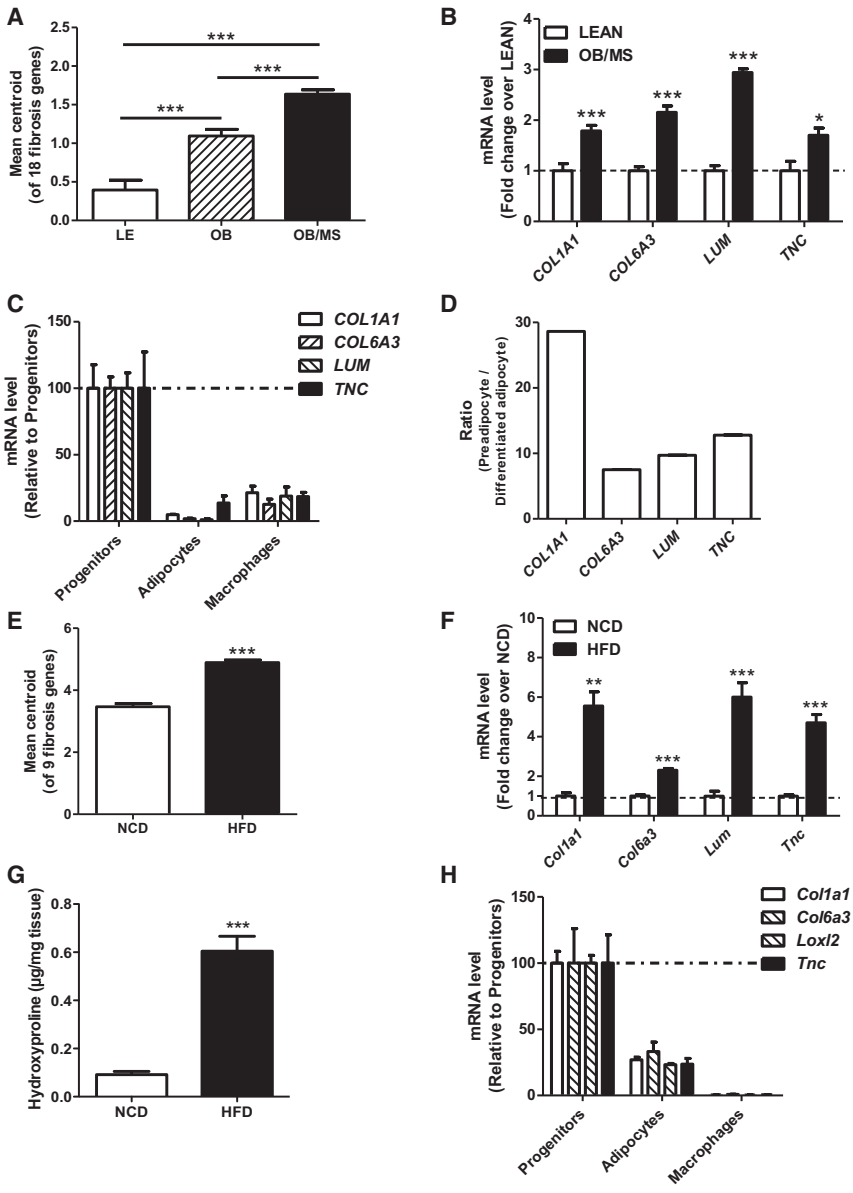

Figure 1. Fibrosis Appearance during Obesity in Adipose Tissues

(A) Centroid analysis of 18 fibrosis pathway genes in subcutaneous adipose tissue from lean (LE), obese (OB), and obese with metabolic syndrome (OB/MS) individuals (n = 8 per group).

(B) mRNA levels of fibrosis genes in adipose tissue from LE and OB/MS individuals (n = 8 per group).

(C) Expression of fibrosis genes in progenitors, adipocytes, and macrophages from human adipose tissue (n = 5 per group).

(D) Changes during human preadipocyte differentiation of extracellular matrix gene expression (n = 9).

(E) Centroid analysis of nine fibrosis pathway genes in mouse adipose tissue (n = 6 per group).

(F) mRNA levels of fibrosis genes in adipose tissue of C3H/HeOuJ mice fed normal chow diet (NCD) and high-fat diet (HFD) for 4 weeks (n = 6 per group).

(G) Hydroxyproline content of epididymal fat in adipose tissue of C3H/HeOuJ mice fed normal chow diet (NCD) and HFD for 8 weeks (n = 6 per group).

(H) Expression of fibrosis genes in progenitors, adipocytes, and macrophages from C3H/HeOuJ mouse adipose tissue after 6 weeks of HFD (n = 6 per group).

Data are presented for human (A–D) and mouse (E–H) adipose tissues. Values represent mean ± SEM. *$p < 0.05$, **$p < 0.01$, ***$p < 0.001$.

See also Figure S1.

RESULTS

Identification of a Mouse Model of AT Fibrosis Mimicking Human Obesity

In human subcutaneous AT, expression of genes involved in fibrosis showed a progression from lean to obese individuals to reach the highest levels in obese patients with metabolic syndrome (Figure 1A; Table S1). A similar pattern was observed in human visceral AT (Figure S1A). Genes encoding ECM proteins, such as collagen type I alpha 1 (*COL1A1*), collagen type VI alpha 3 (*COL6A3*), lumican (*LUM*), and tenascin C (*TNC*), were upregulated in obese patients with metabolic syndrome compared to lean and healthy individuals (Figure 1B). These genes showed high expression in the progenitor cells of AT stromavascular fraction (SVF) (Figures 1C and S1B). Accordingly, there was a downregulation of fibrosis-related gene expression during human adipocyte differentiation (Figure 1D).

In search for a mouse model of progressive AT fibrosis during the development of obesity, we selected the C3H/HeOuJ mouse strain that has been shown to develop fibrosis in other organs, such as kidney and liver (Campbell et al., 2011; Seki et al., 2007). Compared to mice fed chow diet, obese mice fed HFD for 4 weeks showed a higher body weight (27.9 ± 0.4 g versus 35.5 ± 0.5 g, $p < 0.001$) because of a robust increase of fat mass (2.6 ± 0.3 g versus 9.1 ± 0.3 g, $p < 0.001$). The obese mice also showed an upregulation of genes involved in fibrosis,

been the lack of suitable mouse models. Here, we characterized AT fibrosis in humans and mice to determine whether they share similar features. Unlike the commonly used C57BL/6 mice, mice with a C3H background develop AT fibrosis when obesity is induced by high-fat feeding. This prompted us to investigate the role of TLR4 in C3H/HeJ mice (which carry a spontaneous loss of function mutation of TLR4) and in control C3H/HeOuJ mice treated with an inhibitor of TLR4 signaling (Li et al., 2006). To determine whether immune cells expressing TLR4 are instrumental in promoting AT fibrosis, bone marrow transplantation and clodronate-mediated macrophage depletion were performed. The role of the prototypical TLR4 ligand, lipopolysaccharide (LPS), was investigated in vivo using continuous low-dose infusion of the endotoxin and ex vivo in AT explants.

notably those encoding ECM proteins (*Col1a1*, *Col6a3*, *Lum*, and *Tnc*) (Figures 1E and 1F), which are upregulated in obese humans. This upregulation was accompanied by an increase of hydroxyproline content, an indicator of collagen abundance (Figure 1G). In C3H mice, the fibrotic genes were, as in human AT, preferentially expressed in SVF progenitor cells (Figures 1H and S1C). In the commonly used C57BL/6J mouse strain, the upregulation of fibrosis genes in AT was moderate and observed only after HFD of extended duration (15 weeks) (Figure S1D, in comparison to Figure 1F), despite similar gains in weight (27.7 g ± 1.1 g versus 37.6 ± 1.2 g, $p < 0.001$) and fat mass (2.8 ± 0.5 g versus 10.8 ± 0.7 g, $p < 0.001$) compared with those observed in C3H/HeOuJ mice fed HFD for 4 weeks. As in C3H/HeOuJ mice, the fibrotic genes were preferentially expressed in SVF cells compared to mature adipocytes (Figure S1E). Thus, C3H mice represent a proper model for studying AT fibrosis during the development of obesity.

Mutation and Inhibition of TLR4 Protects Mice from HFD-Induced AT Fibrosis

To determine whether TLR4 was involved in AT fibrosis, we compared the expression of genes involved in tissue remodeling in C3H/HeJ mice carrying an inactivating mutation in the *Tlr4* gene (TLR4^{mut} mice) with C3H/HeOuJ wild-type (WT) mice during a 12 week time course of high-fat feeding. In WT mice, mRNA levels of *Col6a3*, *Loxl2*—which catalyzes the formation of crosslinks in collagens and elastin—the matrix metalloprotease *Mmp2*, and other fibrotic genes were upregulated after 4 weeks of high-fat feeding (Figures 2A and S2A). In TLR4^{mut} mice, AT expression of these genes was lower than in WT mice and showed little progression, if any, during the 12 weeks of HFD (Figure 2A). Interestingly, fibrosis gene expression was comparable in AT from WT and TLR4^{mut} mice fed on normal chow diet for 8 weeks, showing the requirement of, and interaction between, TLR4 and HFD-induced expansion of fat mass to induce AT fibrosis (Figure S2B). To confirm that an inactive TLR4 protects from HFD-induced AT fibrosis, the amount of collagens was assessed. Picrosirius staining showed a dramatic increase of collagen deposition and crosslinking in WT epididymal AT from 6 weeks of HFD, whereas TLR4^{mut} mice were totally protected (Figures 2B and 2C; Figures S2C and S2D). This result was confirmed by measurement of hydroxyproline content (Figure 2D). Gene expression on isolated AT progenitors indicated a profibrotic profile in WT mice compared to TLR4^{mut} mice (Figure 2E). We also performed continuous perfusion of a specific inhibitor of TLR4 signaling (TAK242) in HFD-fed WT mice. Inhibition of TLR4 signaling with TAK242 limited collagen deposition (Figure 2F). Therefore, genetic, as well as pharmacological, impairment of TLR4 signaling prevents the development of AT fibrosis.

Fibrosis Is Associated with Adipocyte Metabolic Dysfunction and Death

We also explored the consequences of AT fibrosis on adipocyte morphology, death, and metabolism in fibrosis-prone WT and fibrosis-protected TLR4^{mut} mice. Severe fibrosis in epididymal AT was associated with lower weight of epididymal fat pad in WT mice (Figures 3A and S2C) and was negatively correlated with adipocyte size ($r = -0.45$, $p < 0.001$) (Figure 3B). AT from WT mice had numerous perilipin-negative necrotic adipocytes, whereas those cells were rare in TLR4^{mut} mouse AT (Figure 3C). The higher rate of adipocyte death was associated with higher plasma level of FABP4, a cytosolic fatty acid binding protein released during adipocyte death (Figure 3D).

Fibrosis development was associated with a strong downregulation of genes involved in lipid metabolism in AT from WT mice, whereas no change was observed in AT from TLR4^{mut} mice (Figures S3A). This downregulation was confirmed at the protein level for hormone-sensitive and adipose triglyceride lipases (Figure S3B). As fibrotic AT was characterized by fat cell death and numerous nonadipose cells (Figures 3C and 3E), we pursued metabolic characterization on isolated intact adipocytes. Perilipin-positive adipocytes were slightly smaller, and metabolic gene expression was markedly altered in WT compared to TLR4^{mut} mice (Figures 3F and 3G). In vitro lipolysis experiments on isolated adipocytes showed that basal and stimulated glycerol release was lower in WT, compared to TLR4^{mut}, mice (Figure 3H). Together, these data suggest a negative association between fibrosis and adipocyte function.

Mutation of TLR4 Protects Mice from HFD-Induced AT Macrophage Response

During the development of HFD-induced obesity, expression of macrophage genes, including *Emr1* encoding the specific marker of macrophages (F4/80), was increased in WT mouse AT (Figure 4A). The increase was delayed and moderate in TLR4^{mut} mice. The number of crown-like structures was much higher in WT, compared with TLR4^{mut}, mouse AT (Figure 4B). Consistently, flow cytometry analysis performed at 8 weeks of HFD revealed a higher number of AT macrophages in WT mice (2.2-fold, $p < 0.001$) compared to TLR4^{mut} mice (Figure 4C). These AT macrophages were in majority M2 (CD45+/CD11b+/F4/80+/CD11c-/CD206+) and M2-like (CD45+/CD11b+/F4/80+/CD11c-/CD206-) macrophages (Figure 4D) and were expressed at higher levels in WT mice fed HFD than in those fed normal chow diet (Figures S4A and S4B). Gene expression performed on isolated macrophages showed higher activation in WT, compared to TLR4^{mut}, mice (Figure 4E). As mast cells accumulate in inflamed and fibrotic human fat depots (Divoux et al., 2012), we investigated the number and location of these cells in AT from TLR4^{mut} and WT mice. Mast cells were more numerous in WT, compared to TLR4^{mut}, mice (Figure S4C). Nevertheless, mast cells were located outside fibrotic areas, and their number was very low in comparison to AT macrophages (Figure S4D).

The relationship between AT macrophage activation and fibrosis was shown by the strong positive correlation between mRNA expression of *Emr1* and *Col6a3* ($r = 0.60$, $p < 0.001$) (Figure 4F). AT gene expression of the major profibrotic factor transforming growth factor beta 1 (*Tgfb1*) was upregulated after 4 weeks of HFD in WT mice (Figure 4G). There were strong correlations between *Tgfb1* and *Emr1* mRNA expression ($r = 0.95$ $p < 0.001$) (Figure 4H) and between *Tgfb1* and *Col1a1* or *Col6a3* mRNA expression ($r = 0.74$ $p < 0.001$; $r = 0.43$ $p < 0.01$) (Figure S4E). Gene expression of the TLR4-downregulated

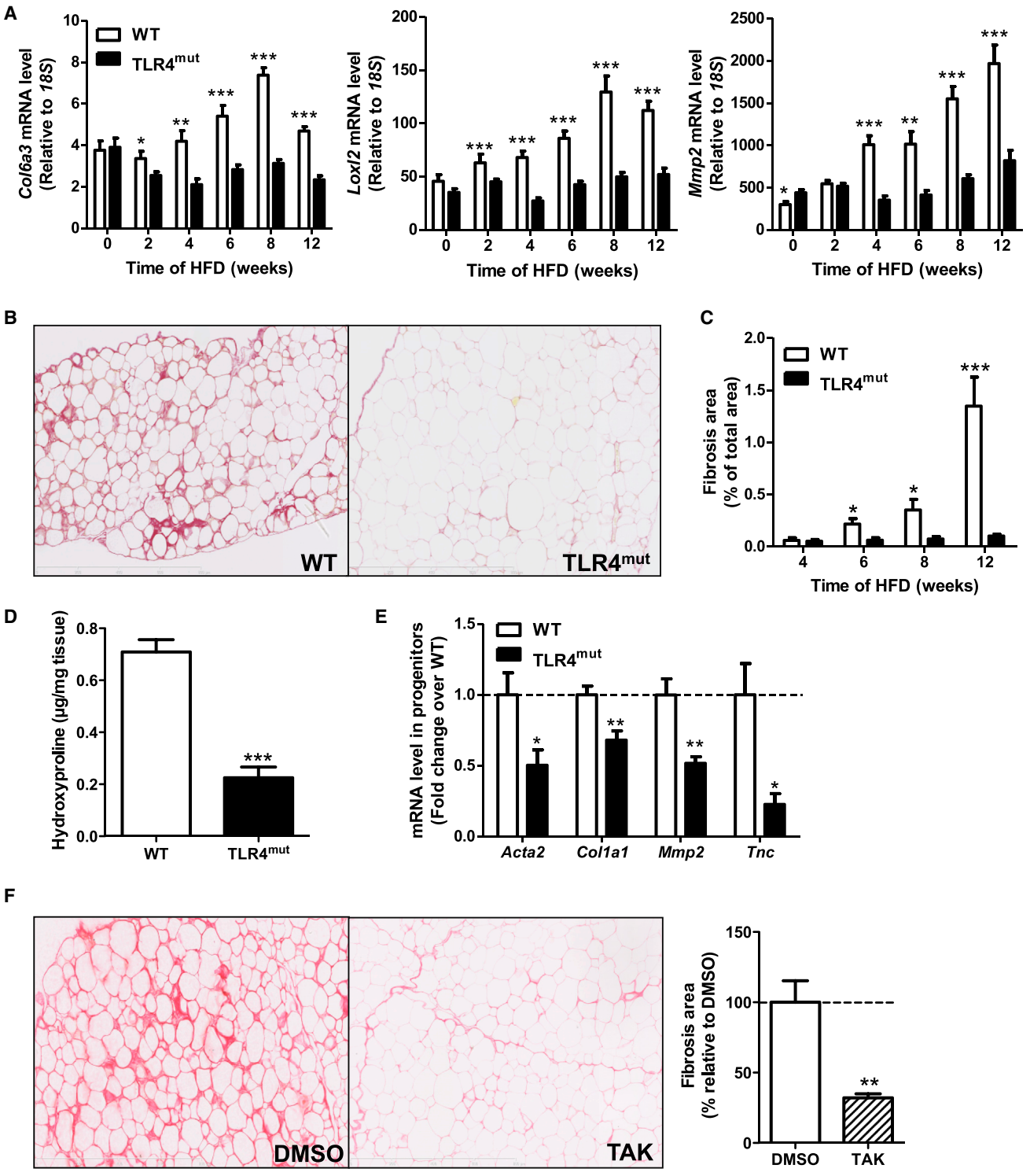

Figure 2. Time Course Study Shows Development of Fibrosis in Wild-Type, but not in TLR4^{mut}, Mouse Adipose Tissue during High-Fat Diet

(A) mRNA levels of fibrosis genes during high-fat diet (HFD) in wild-type (WT) and TLR4^{mut} epididymal adipose tissue (n = 8 per group).

(B) Representative picrosirius red slides (×100) showing collagen fiber deposition at 12 weeks of HFD.

(C) Quantitation of fibrosis area at different time points (n = 8 per group).

(D) Determination of epididymal fat collagen content by hydroxyproline assay at 12 weeks of HFD (n = 7 per group).

(E) Fibrosis gene expression in progenitors from WT and TLR4^{mut} mice at 6 weeks of HFD (n = 6 per group).

(legend continued on next page)

TGF-β pseudoreceptor, *Bambi*, was lower in WT, compared with TLR4^{mut}, mouse AT (Figure S4F).

Macrophage activation and fibrosis were not general features among tissues from HFD-fed WT mice. In subcutaneous fat, there was no evidence of fibrosis (Figures S5A and S5B) and macrophage activation (Figure S5C), unlike in perirenal fat, an intraabdominal depot behaving like epididymal fat (Figure S5D). In liver, fibrosis was not observed after high-fat feeding (Figures S5E and S5F).

HFD-Induced AT Fibrosis Is Dependent on Immune Cell Toll-like Receptor 4 and Macrophages

To investigate the involvement of immune cells in the genesis of AT fibrosis, TLR4^{mut} mice were irradiated. Bone marrow transplantation (BMT) of control or mutated mouse donor cells was performed into irradiated TLR4^{mut}-recipient mice (BMT-WT and BMT-TLR4^{mut} mice). The experiment did not alter hematopoietic cell lineage distribution in blood. Monocyte, lymphocyte, and granulocyte counts were similar in the two types of chimeric mice (Figure S6A). In BMT-WT mice, an intact *Tlr4* gene was detected in blood-hematopoietic-derived cells and in AT macrophages (Figure S6B). At 8 weeks of HFD, TLR4^{mut} mice reconstituted with WT bone marrow had higher AT expression of *Tgfb1*, *Col6a3*, and vimentin (*Vim*) genes compared to BMT-TLR4^{mut} mice (Figure 5A). Picrosirius staining showed higher collagen deposition in AT from BMT-WT mice compared to BMT-TLR4^{mut} mice (Figure 5B). Associated to fibrosis, there was higher AT expression of *Tnf*, *Ccl2*, and *Mrc1* macrophage genes (Figure 5C).

To confirm the involvement of macrophages, we performed injections of liposomes containing clodronate in WT mice fed HFD. Clodronate induced a reduction of the macrophage marker *Emr1* and fibrosis gene mRNA levels, as well as a decrease in hydroxyproline content (Figures 5D–5F).

Insulin Resistance Is Associated with Immune TLR4-Mediated AT Fibrosis

The relationship between insulin resistance and AT fibrosis was investigated in humans and in mice. The quantitative insulin sensitivity check index (QUICKI) decreased from lean to obese individuals and reached the lowest levels in obese patients with metabolic syndrome (Figure 6A). QUICKI values were negatively correlated with fibrosis gene expression ($r = -0.8$, $p < 0.001$) (Figure 6B).

TLR4 mutation prevented the HFD-induced decrease in insulin tolerance (Figure 6C). This improvement was not related to difference in weight gain during HFD between WT and TLR4^{mut} mice. WT mice were more insulin-resistant, i.e., had lower QUICKI values, than did TLR4^{mut} mice (0.28 ± 0.01 versus 0.42 ± 0.01, $p < 0.001$). QUICKI values were negatively correlated to the extent of AT fibrosis ($r = -0.52$, $p < 0.001$) (Figure 6D).

HFD-fed BMT-WT mice were less glucose tolerant than were BMT-TLR4^{mut} mice (Figure 6E). The insulin × glucose product at 15 min after glucose injection correlated with the extent of AT fibrosis ($r = 0.6$, $p < 0.01$) (Figure 6F).

The TLR4 Ligand LPS Induces AT Fibrosis through TGFβ1

To assess if LPS induces AT fibrosis, we performed continuous perfusion of LPS for 4 weeks in chow-diet-fed WT mice. This treatment induced a 2-fold increase in LPS plasma level (Figure 7A), with no change in body weight (Figure S7A). LPS perfusion increased expression of several fibrotic genes (Figures 7B and S7B) and surface of fibrotic areas in AT (Figure 7C). AT macrophage gene expression was also higher (Figure S7C), together with the number of AT macrophages, chiefly of M2 and M2-like phenotypes, and lymphocytes (Figures 7D and 7E).

To clarify the role of TGFβ1 in LPS-induced AT fibrosis, we performed ex vivo experiments. AT explants treated with LPS showed an increase of macrophage and fibrosis gene expression. Addition of a neutralizing antibody against TGFβ1 blocked the effect of LPS on fibrosis gene expression but had only a limited effect on *Tnf* gene expression (Figures 7F and 7G).

DISCUSSION

In humans, AT expression of fibrosis-related genes was increased in obesity and further elevated when obesity and metabolic syndrome were combined. We identified C3H mice fed HFD as a suitable model of human obesity-induced AT fibrosis. In both humans and mice, the extent of AT fibrosis was linked to the worsening of insulin resistance. Time course studies in C3H mice revealed that AT expansion was associated with collagen overproduction, tissue remodeling macrophage response, and adipocyte metabolic dysfunction and death. Investigation of mice with genetic and pharmacological inhibition of TLR4 signaling showed that this endotoxin receptor is essential in mediating the development of AT fibrosis. Bone marrow transplantation experiments, clodronate-induced depletion of macrophages, and LPS infusion demonstrated that activation of macrophage TLR4 is central in AT fibrogenesis and that this process involves the profibrotic factor TGFβ1.

The C57BL/6J strain, traditionally used in obesity research, appeared, at first glance, as the model of choice to study AT fibrosis in mice. However, when fed HFD, these mice presented a late and modest modulation of profibrotic gene expression (Kwon et al., 2012). This moderate development of AT fibrosis may be related to lower immune cell infiltration during HFD compared to C3H mice (Nguyen et al., 2007; Spencer et al., 2010). The C3H mouse strain represents a more appropriate model as upon HFD these mice overexpress the same genes encoding ECM proteins as those upregulated during human obesity. In both obese individuals and obese C3H mice, genes related to fibrosis were preferentially expressed in progenitor cells, in line with this cell type being the major matrix producer in AT (Keophiphath et al., 2009; Lacasa et al., 2007). Time course

(F) Representative picrosirius red slides (×100) after treatment with vehicle (DMSO) or TAK242 in WT mice and quantitation of fibrosis area at 8 weeks of HFD ($n = 10$ per group).

Values represent mean ± SEM. *$p < 0.05$, **$p < 0.01$, ***$p < 0.001$.

See also Figure S2.

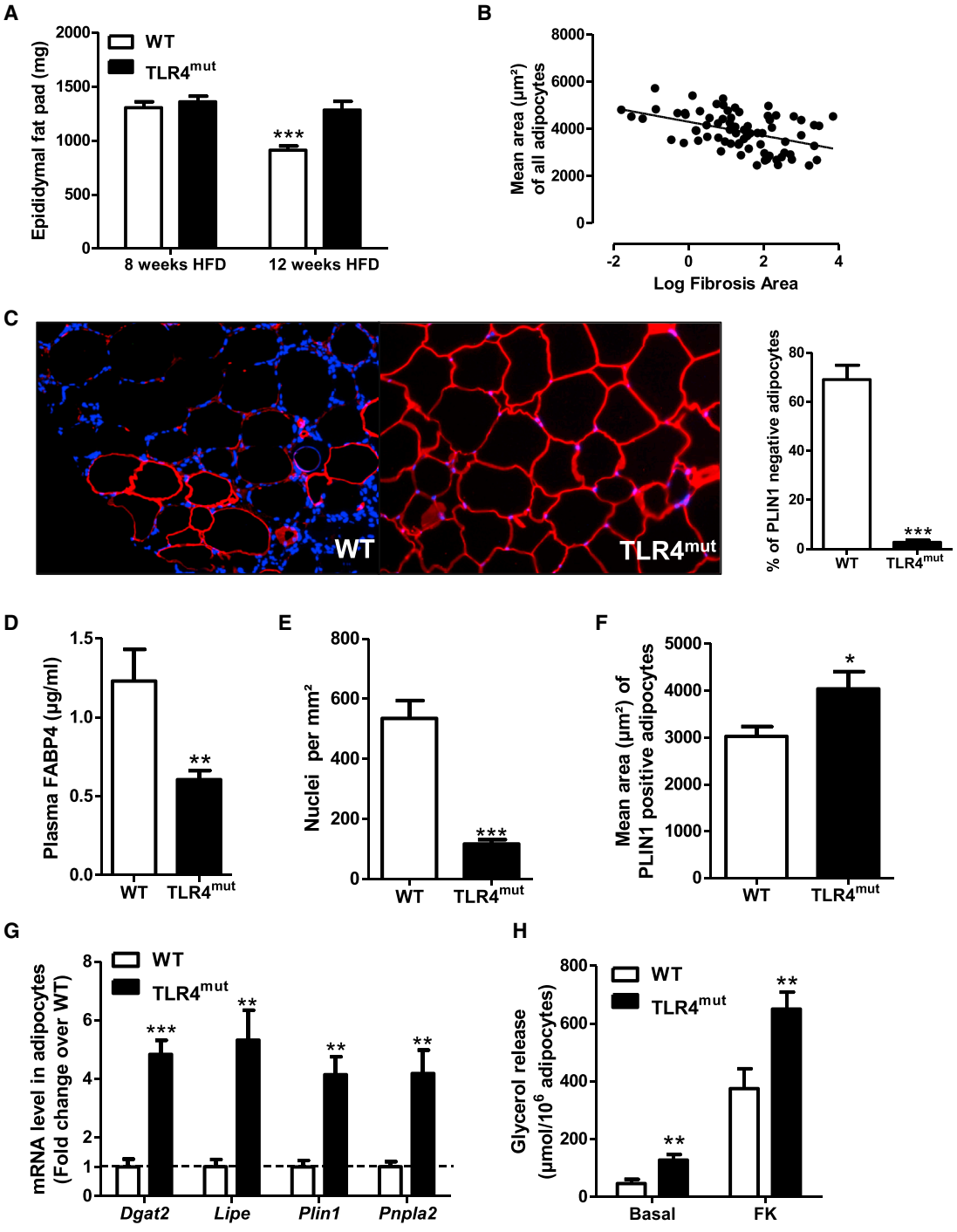

Figure 3. High-Fat Diet Induces Adipocytes Death and Metabolic Alterations in Adipocytes from Wild-Type, but not TLR4^{mut}, Mice

(A) Epididymal fat-pad weight at 8 and 12 weeks of high-fat diet (HFD) in wild-type (WT) and TLR4^{mut} mice (n = 8 per group).

(B) Correlation between mean area of adipocytes and area of fibrosis determined by picrosirius staining.

(C) Representative immunofluorescence of perilipin 1(PLIN1) staining (×200) and quantitation of PLIN1-negative cells at 12 weeks of HFD (n = 8 per group).

(D) Plasma fatty acid binding protein 4 (FABP4) level after 12 weeks of HFD (n = 8 per group).

(E) Number or nuclei per mm^2 at 12 weeks of HFD (n = 8 per group).

(F) Mean area of PLIN1-positive cells at 12 weeks of HFD (n = 8 per group).

(G) Metabolic gene expression in isolated adipocytes at 6 weeks of HFD (n = 6 per group).

(H) Glycerol release during basal and forskolin (FK)-stimulated in vitro lipolysis experiments on isolated adipocytes at 8 weeks of HFD (n = 6 per group).

Values represent mean ± SEM. *p < 0.05, **p < 0.01, ***p < 0.001. See also Figure S3.

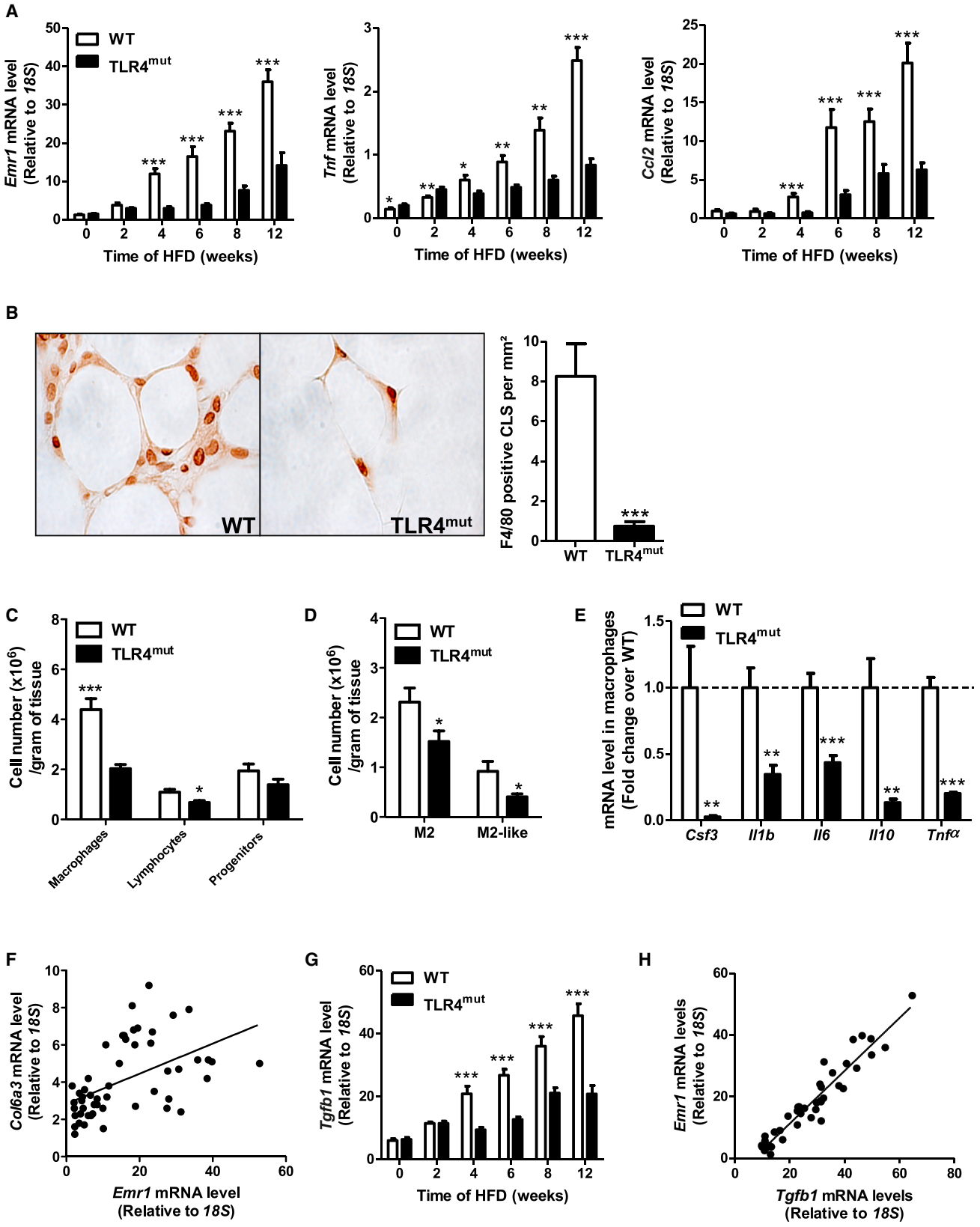

(legend on next page)

Please cite this article in press as: Vila et al., Immune Cell Toll-like Receptor 4 Mediates the Development of Obesity- and Endotoxemia-Associated Adipose Tissue Fibrosis, Cell Reports (2014), http://dx.doi.org/10.1016/j.celrep.2014.03.062

studies revealed increased gene expression of two major collagen species within AT, *Col1a1*, and *Col6a3*, resulting in collagen accumulation and crosslinking. Fibrosis gene expression was not increased in C3H mice fed chow diet, indicating that AT expansion and consequent remodeling is a prerequisite for the development of AT fibrosis. During diet-induced obesity, there was, however, no evidence of fibrosis in the liver, revealing that different conditions trigger the appearance fibrosis in the two organs.

In wound healing, there is an intimate link between fibrosis and inflammation (Stramer et al., 2007). In AT, flow cytometry and immunohistochemistry showed a higher amount of immune cells, notably macrophages, and macrophage marker gene expression. Macrophages are seen in several organs as master regulators of fibrosis (Wynn and Barron, 2010). Flow cytometry analyses showed that alternatively activated M2 was the dominant AT macrophage subset, and M2-like was the most induced by HFD in our model (Klimcakova et al., 2011a; Morris et al., 2011; Zeyda et al., 2010). M2 and M2-like macrophages are involved in tissue repair. Gene expression of macrophage markers correlated with that of collagens as observed in human AT (Spencer et al., 2010). Macrophage depletion induced a reduction of fibrosis-related gene expression and hydroxyproline content, indicating a causal link between macrophage activation during HFD and AT fibrosis. In vitro, human macrophages impair adipogenesis and promote a profibrotic phenotype in preadipocytes (Keophiphath et al., 2009; Lacasa et al., 2007). Our data point to macrophages as essential players in the development of AT fibrosis by preadipocytes.

There is mounting evidence that AT fibrosis is linked to metabolic dysfunction (Sun et al., 2013). At whole-tissue level, there was a decrease of epididymal fat-pad weight and fat cell size at 12 weeks of HFD in WT mice. Accordingly, we showed a negative correlation already reported in human AT between the extent of fibrosis and adipocyte size (Divoux et al., 2010). We also found a much higher proportion of dead adipocytes in fibrotic AT (Cinti et al., 2005; Strissel et al., 2007). Patterns of metabolic gene expression suggested AT metabolic dysfunction in surviving fat cells. As a representative function, AT from obese WT mice was characterized by impaired basal and stimulated lipolysis. These results reveal an intricate combination of AT fibrosis, macrophage activation, and adipocyte dysfunction and death that may contribute to the metabolic complications of obesity. The strongest signature of genes encoding ECM proteins was found in obese patients with metabolic syndrome, as also observed in morbidly obese patients, indicating a link between AT fibrosis and worsening of the metabolic status (Henegar et al., 2008). This was corroborated by the positive association between AT fibrosis and insulin resistance found both in mice and humans.

TLR4 is a key initiator of macrophage response and a modulator of systemic insulin sensitivity (Saberi et al., 2009; Tsukumo et al., 2007). Here, we show that obese TLR4^{mut} mice are protected from AT fibrosis. During HFD, there was no induction of gene expression and no evidence for deposition of collagens in AT. Gene expression of *Mmp2* and *Mmp9* encoding macrophage matrix metalloproteases and the established profibrotic factor *Tgfb1* were upregulated in WT, but not in TLR4^{mut}, mice. Among other functions in tissue remodeling, matrix metalloproteases activate cathepsin-based proteolytic pathways to generate an active TGFβ1. TGFβ family members produced by macrophages mediate a fibrotic reaction in human AT progenitor cells in vitro (Bourlier et al., 2012; Keophiphath et al., 2009). Our data support the role of TGFβ1 and matrix metalloproteases in AT fibrogenesis in vivo as shown in other tissues (Biernacka et al., 2011; Pardo and Selman, 2006). BMT revealed that TLR4-competent immune cells in AT restore the HFD-mediated induction of collagen accumulation and upregulation of macrophage markers, ECM, and profibrotic genes. Of note, irradiated WT mice transplanted with bone marrow of TLR4 null mice show markedly reduced monocyte infiltration in AT (Saberi et al., 2009). Furthermore, treatment with a TLR4 signaling inhibitor protected mice against fibrosis during HFD. Together, these results show that AT hematopoietic cell TLR4 is essential for recruitment and activation of macrophages, leading to AT fibrosis.

Obesity has been linked to metabolic endotoxemia with an elevation of circulating LPS levels (Cani et al., 2007). LPS is considered as the most potent inducer of TLR4. We show that a moderate increase in LPS plasma levels is sufficient to induce AT macrophages and fibrosis. Activation of TLR4 by LPS also induced fibrosis in AT ex vivo. Neutralization of the profibrotic factor, TGFβ1, completely prevented the induction of fibrosis, suggesting a direct link between the activation of TLR4 by LPS and AT fibrosis mediated by TGFβ1.

Fibrosis, macrophage activation, and adipocyte dysfunction constitute a detrimental triptych in AT. We found that these intricate processes are dependent on TLR4 expressed in AT macrophages. LPS, the main TLR4 ligand, whose plasma levels are increased during obesity-associated metabolic endotoxemia, is a likely trigger of AT fibrogenesis. The TLR4-dependent AT remodeling leads to limited fat expansion and fibrosis and low metabolic capacity and necrotic death of fat cells, which concur to the metabolic complications of obesity.

Figure 4. Time Course Study Shows Development of Macrophage Infiltration and Activation in Wild-Type, but not in TLR4^{mut}, Mouse Adipose Tissue during High-Fat Diet

(A) mRNA levels of inflammatory genes during high-fat diet (HFD) in wild-type (WT) and TLR4^{mut} adipose tissue (n = 8 per group).
(B) Representative staining (×1,000) and quantitation of F4/80-positive crown-like structures (CLS) (n = 8 per group).
(C) Quantitation of stromavascular fraction cell types by flow cytometry at 8 weeks of HFD (n = 8 per group).
(D) Adipose tissue macrophage phenotyping by flow cytometry at 8 weeks of HFD (n = 8 per group).
(E) Gene expression in macrophages of WT and TLR4^{mut} mice at 6 weeks of HFD (n = 6 per group).
(F) Correlation between *Emr1* and *Col6a3* mRNA levels.
(G) mRNA levels of a major profibrotic factor *Tgfb1* (n = 8 per group).
(H) Correlation between *Emr1* and *Tgfb1* mRNA levels.
Values represent mean ± SEM. *p < 0.05, **p < 0.01, ***p < 0.001. See also Figures S4 and S5.

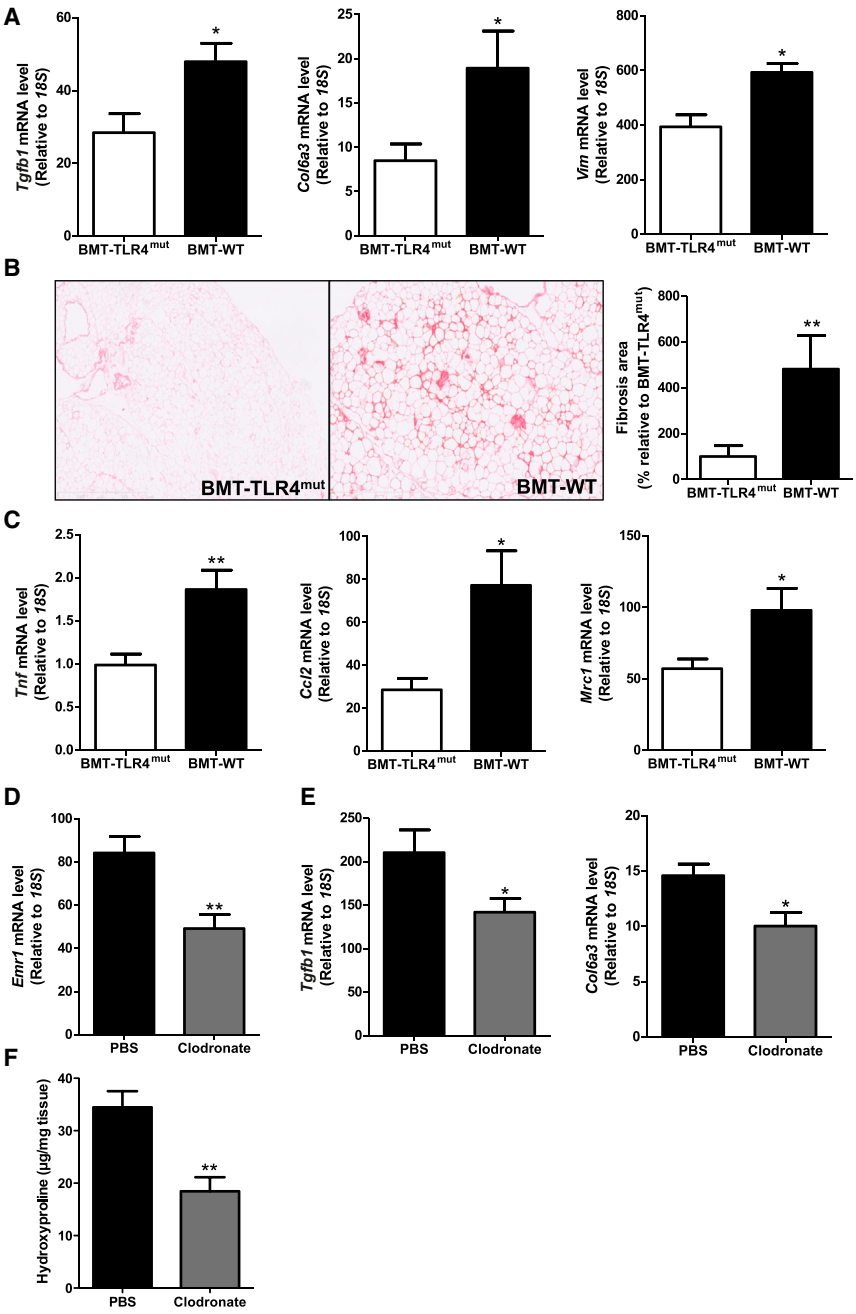

Figure 5. Role of Immune Cell TLR4 and Macrophages in the Induction of Fibrosis in Adipose Tissue

Bone marrow transplantation (BMT) of donor cells from wild-type (WT) or mutated TLR4 (TLR4^{mut}) mouse was performed into irradiated recipient TLR4^{mut} mice (BMT-TLR4^{mut} and BMT-WT mice). Mice were analyzed after 8 weeks of HFD.

(A) mRNA levels of fibrosis genes in BMT experiment (n = 8 per group).

(B) Representative picrosirius red slides (×100) showing collagen fiber deposition and quantitation of fibrosis area at 8 weeks of HFD (n = 8 per group).

(C) mRNA levels of macrophage genes (n = 8 per group).

(D) mRNA levels of the macrophage marker *Emr1* (F4/80) in PBS- and clodronate-treated mice (n = 12 per group).

(E) mRNA levels of fibrosis-related genes in PBS- and clodronate-treated mice (n = 12 per group).

(F) Determination of hydroxyproline content in adipose tissue at 8 weeks of HFD in PBS- and clodronate-treated mice (n = 6 per group).

Values represent mean ± SEM. *p < 0.05, **p < 0.01. See also Figure S6.

EXPERIMENTAL PROCEDURES

Expression of Human Fibrosis Genes in Human AT

Clinical studies were approved by the Ethics Committee of the Third Faculty of Medicine, Charles University, Prague. AT samples were obtained from carefully phenotyped lean, obese, and obese with metabolic syndrome individuals (Klimcakova et al., 2011a, 2011b). Adipocytes and SVF were isolated from subcutaneous AT by collagenase digestion (Klimcakova et al., 2011a). Progenitor cells from the SVF were differentiated as previously reported (Rossmeislová et al., 2013). Gene expression profiling was performed using whole-genome 44k oligonucleotide arrays (Agilent Technologies) (Klimcáková et al., 2011b).

Animals

Animal protocols were performed in accordance with French and European Animal Care Facility guidelines. Five-week-old male C3H/HeJ and C3H/HeOuJ mice were purchased from the Jackson Laboratory. C57BL/6J mice were from Elevage Janvier.

Diets

After weaning, C3H/HeJ and C3H/HeOuJ mice were fed with HFD (45% energy as fat, Research Diets D12451) for 2 to 12 weeks. In some experiments, C3H/HeOuJ mice were fed normal chow diet (10% energy as fat, Research Diets D12450B) for 4 weeks. C57BL/6J mice were fed normal chow and HFD for 15 weeks.

Body Composition

Mouse body composition was evaluated by quantitative nuclear magnetic resonance imaging (EchoMRI 3-in-1 system; Echo Medical Systems).

Glucose and Insulin Tolerance Tests

Mice were fasted for 6 hr with free access to drinking water. Glucose was administered intraperitoneally (1 g/kg), and blood glucose levels were monitored from the tip of the tail with a glucometer (Accucheck, Roche). At 15 min after glucose injection, blood was collected for insulin quantitation. For insulin tolerance tests, insulin was administered intraperitoneally (0.6 mU/g), and blood glucose was measured at various times after injection.

Generation of Bone Marrow Chimeras

C3H/HeJ mice at 10 weeks of age received a sublethal dose of whole-body irradiation (9 Gy). The day after irradiation, donor C3H/HeJ or C3H/HeOuJ mice were killed, and their femurs and tibias were removed aseptically. Marrow cavities were flushed, and single-cell suspensions were prepared. The irradiated recipients received 1 × 10^7 bone marrow cells in 0.1 ml of PBS by retro-orbital injection. During 4 weeks after BMT, Bactrim (Roche)

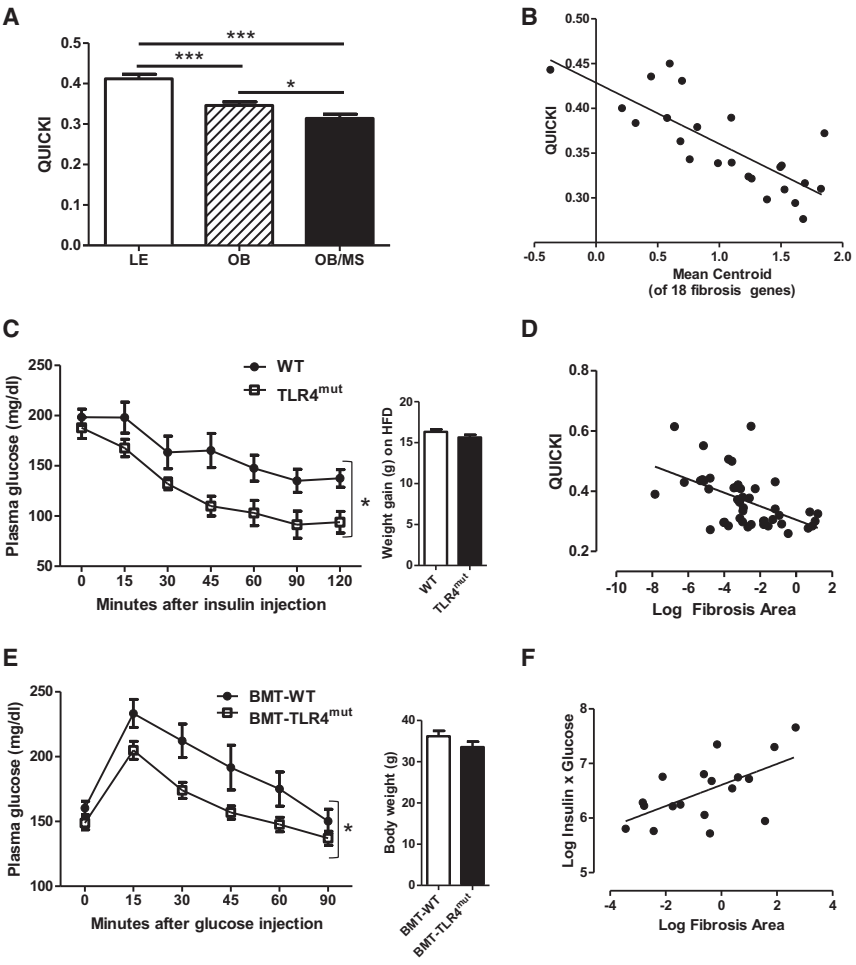

Figure 6. Insulin Sensitivity Is Associated with Adipose Tissue Fibrosis in Humans and Mice

(A) Quantitative insulin sensitivity check index (QUICKI) values in lean (LE), obese (OB), and obese with metabolic syndrome (OB/MS) individuals (n = 8 per group).

(B) Correlation between QUICKI and mean centroid of 18 fibrosis pathway genes in humans.

(C) Insulin tolerance test and weight gain after 8 weeks of high-fat diet in wild-type (WT) or mutated TLR4 ($TLR4^{mut}$) mice (n = 8 per group).

(D) Correlation between QUICKI and quantitation of fibrosis area by picrosirius staining in mice.

(E) Glucose tolerance test and body weight after 8 weeks of high-fat diet in bone-marrow-transplanted (BMT) mice (n = 8 per group). See also Figure 5.

(F) Correlation between insulin × glucose levels determined at 15 min after glucose injection and quantitation of fibrosis area by picrosirius staining in BMT mice.

Values represent mean ± SEM. *p < 0.05, ***p < 0.001

was added to drinking water. After 2 additional weeks, mice were switched to HFD. Mice were killed 8 weeks later to collect blood and tissues.

LPS and TAK242 Continuous Infusions

For LPS infusion, 5-week-old mice fed normal chow diet were implanted intraperitoneally with an osmotic minipump (Alzet Model 1004). Pumps were filled either with NaCl (0.9%) or LPS (from *Escherichia coli* 055:B5; Sigma) to infuse 300 μg $kg^{-1} \cdot day^{-1}$ for 4 weeks.

For TAK242 infusion, mice were fed HFD for 4 weeks and then implanted intraperitoneally with osmotic minipumps filled either with a solution of DMSO/ethanol/H_2O (5/1.5/3.5) or TAK242 (Invivogen) to infuse 350 μg $kg^{-1} \cdot day^{-1}$ for 4 weeks during HFD feeding.

Macrophage Depletion by Liposome-Encapsulated Clodronate

C3H/HeOuJ mice were fed HFD and concomitantly received intraperitoneally 250 μl liposomes containing clodronate (5 mg/ml) or an equivalent volume of liposomes containing PBS once per week for 8 weeks (Dr van Rooijen, Vrije Universiteit).

Analysis of Blood Parameters

Plasma glucose levels were measured by an enzymatic assay kit (Glucose RTU, Biomerieux). Serum insulin concentration was determined by an enzyme-linked immunosorbent assay (Mouse Ultrasensitive Insulin ELISA, ALPCO Diagnostics). Plasma LPS levels were measured through the quantitation of 3-β-hydroxymyristate (Nguyen et al., 2013). Plasma FABP4 concentration was determined by enzyme immunoassay (BioVendor, R&D).

In Vitro Lipolysis Experiments

Isolated packed adipocytes were diluted and incubated in Krebs-Ringer bicarbonate buffer with 2% fatty acid-free BSA and 1 g/l glucose containing forskolin (10^{-5} M) for maximal lipolysis determination. Glycerol was measured by free glycerol reagent (Sigma). Total lipid content was determined gravimetrically after organic extraction.

Explant Protocol

Epididymal fat pad of C3H/HeOuJ mice at 6 weeks of HFD was dissected, cut into small pieces, distributed in well plates containing ECBM (PromoCell) supplemented with 0.1% fatty acid-BSA, and incubated at 37°C with 5% CO_2 for 1 hr. AT was then treated with 100 ng/ml LPS (Invivogen) or NaCl in the presence of a neutralizing antibody against TGFβ1 (1 μg/ml) for 24 hr or a immunoglobulin G (IgG) isotype control (R&D Systems). At the end of the incubation period, AT was frozen in liquid nitrogen and stored at −80°C.

Flow Cytometry Analysis, Immunophenotyping, and Cell Sorting

Fat pads were digested by a cocktail of collagenases. Digested tissues were filtered through a 225 μm pore filter. SVF was separated from remaining fibrous material and floating adipocytes by centrifugation at 300 × *g*. SVF cells were then filtered through a 70 μm pore filter and incubated in an erythrocyte lysing buffer. Cells (10^6) were incubated 10 min at room temperature with Fcblock (BD Biosciences) in flow cytometry buffer (PBS, 0.2% BSA, 2 mM EDTA). For flow cytometry analysis, pools of specific fluorescent-labeled antibodies (PerCP-CD45, FITC-F4/80, APC-Cy7-CD11b, PE-Cy7-CD11c, PE-CD206, APC-CD31, PE-CD34, FITC-Sca1, PE-CD3, FITC-CD4, and APC-CD8 from BD Biosciences) were prepared and added to the SVF solution. After an incubation of 30 min on ice in the dark, cells were washed with 2 ml of PBS and centrifuged at 300 × g, 10 min at 4°C. Supernatant was discarded, and the cell pellet was resuspended in 0.5 ml of PBS.

For cell sorting, pools of specific fluorescent-labeled antibodies (PerCP-CD45, PE-F4/80, APC-CD31, and Brilliant Violet-Sca1 from BD Biosciences) were prepared and added to the SVF solution. After 30 min incubation on ice, cells were washed with 2 ml of cold PBS and centrifuged at 300 × g, 10 min at 4°C. Supernatant was discarded, and the cell pellet was

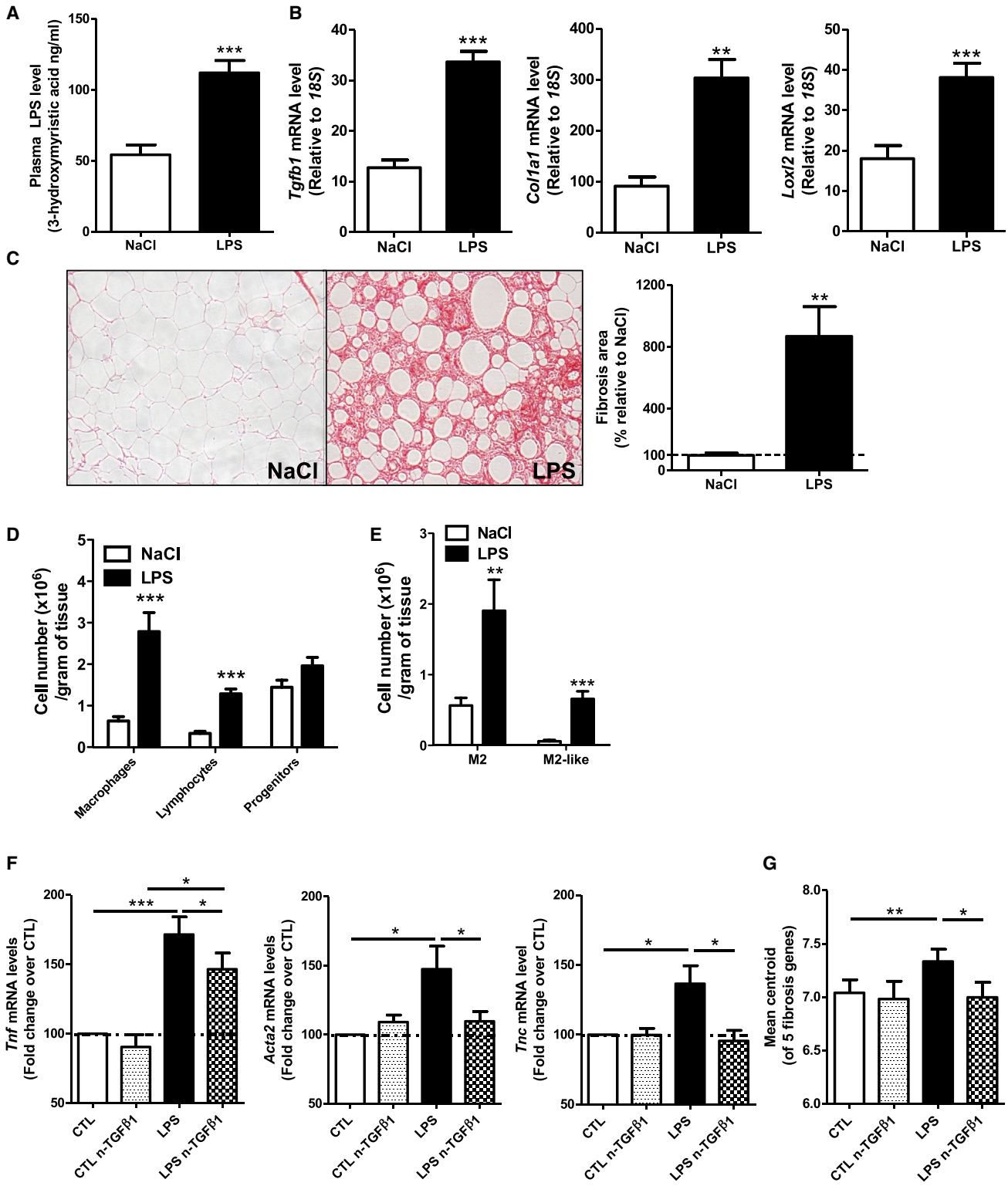

Figure 7. Lipopolysaccharide Treatment Promotes Adipose Tissue Fibrosis via the TGFβ1 Pathway

(A) Fasting plasma lipopolysaccharide (LPS) levels after 4 weeks of NaCl or LPS infusion (n = 9 per group).

(B) mRNA levels of fibrosis genes after 4 weeks of NaCl or LPS infusion (n = 9 per group).

(C) Representative picrosirius red slides (×100) showing collagen fiber deposition and quantitation of fibrosis area.

(legend continued on next page)

Please cite this article in press as: Vila et al., Immune Cell Toll-like Receptor 4 Mediates the Development of Obesity- and Endotoxemia-Associated Adipose Tissue Fibrosis, Cell Reports (2014), http://dx.doi.org/10.1016/j.celrep.2014.03.062

resuspended in 1 ml of PBS. Macrophages stained with PerCP-C45 and PE-F4/80 were separated from progenitors stained with Brilliant Violet-Sca1 using a fluorescence-activated cell sorter. Macrophages and progenitor cells were collected and immediately frozen for gene expression analysis.

RNA Extraction and Real-Time PCR

Total RNA was extracted using RNeasy or RNeasy Micro Kits (QIAGEN). RNA was quantified by Nanodrop spectrophotometer (ND-1000, Nanodrop Technologies). RNA (200 ng to 1 μg) was reverse transcribed using the Multi-Reverse Transcriptase Kit (Invitrogen). mRNA levels were measured by quantitative RT-PCR using Applied Biosystems StepOne or the Fluidigm Biomark system (Viguerie et al., 2012). Taqman probes were provided by Applied Biosystems. SYBR Green primers are listed in Table S2.

Western Blot Analysis

AT were homogenized using the Precellys 24 apparatus (Bertin) in a buffer containing 50 mM Tris-HCl (pH 8.0), 150 mM NaCl, 1% NP40, 0.5% Sodium deoxycholate, 0.1% SDS, 10 μl/ml protease inhibitor, 10 μl/ml phosphatase I inhibitor, and 10 μl/ml phosphatase II inhibitor. Tissue lysates were centrifuged at 14,000 g for 30 min at 4°C, and supernatants were stored at −80°C. Solubilized proteins (30 μg) from AT were run on 4%–12% gradient SDS-PAGE (Biorad) transferred onto nitrocellulose membrane (Hybond ECL, Amersham Biosciences) and incubated with primary antibodies against ATGL and HSL (Cell Signaling Technology). Subsequently, immunoreactive proteins were determined by chemiluminescence (SuperSignal West Dura Thermo Scientific). For loading controls, proteins were detected directly with the Criterion Stain Free Gel Imaging System (BioRad).

Histological Analysis

AT was fixed with neutral-buffered formalin 10% for 24 hr, embedded in paraffin, sectioned, and stained with picrosirius dye. Fibrosis quantification was performed after picrosirius staining using ImageJ.

For mast cells staining, slides were stained in toluidine blue solution (Sigma). Mast cells were counted on the basis of metachromatic staining of their cytoplasmic granules by toluidine blue.

Immunohistochemistry and Immunofluorescence

For immunofluorescence, AT serial sections were incubated overnight at room temperature in a humid chamber with anti-perilipin antibody (GP 29 Progen) diluted at 1:200 in a solution containing 0.1% of BSA and 0.05% of Tween 20. After three washes in PBS, immunofluorescence was detected following incubation with Alexa Fluor 568 anti-guinea pig diluted at 1:200. For nucleus staining, Hoechst 33342 (5 μg/ml) was added to section and stained for 5 min at room temperature. Slides were mounted and processed for microscope observation.

For immunohistochemistry, adipose fat serial sections were incubated overnight at room temperature in a humid chamber with anti-F4/80 antibody (AbD serotec) diluted at 10 ng/μl. After three washes in TBS buffer, incubation for 1 hr in the appropriate secondary biotinylated antibody was performed. Staining was revealed with diaminobenzidine (DAB 1%).

Hydroxyproline Assay

Frozen AT (100 mg) was heated in 6 N HCl at 120°C for 4 hr in sealed tubes. The samples were centrifuged, and 10 μl of supernatant was mixed with 100 μl of chloramine-T solution (1.4% chloramine-T, 10% N-propanol, and 80% citrate-acetate buffer). This mixture was incubated for 20 min at room temperature. Ehrlich's solution was added, and the samples were incubated at 65°C for 20 min. The absorbance was read at 540 nm, and the concentration was determined by the standard curve created by cis-4-hydroxy-L-proline (Sigma-Aldrich).

Statistical Analysis

All statistical analyses were performed using GraphPad Prism (v. 5.0) for Windows (GraphPad Software). Normal distribution of the data was tested with Kolmogorov-Smirnov tests. Paired or unpaired Student's t tests were performed to determine differences between groups. Two-way ANOVA, followed by Bonferroni's post hoc tests, was applied when appropriate. Pearson correlations were applied when data were normally distributed, and Spearman correlations were applied for nonparametric data. All values in figures and tables are presented as mean ± SEM. Statistical significance was set at $p < 0.05$.

SUPPLEMENTAL INFORMATION

Supplemental Information includes Supplemental Experimental Procedures, seven figures, and two tables and can be found with this article online at http://dx.doi.org/10.1016/j.celrep.2014.03.062.

ACKNOWLEDGMENTS

We thank E. Mouisel (UMR 1048) for outstanding help and critical reading of the manuscript. I.K.V. was supported by fellowships from Inserm and Région Midi-Pyrénées. This work was supported by grants from Agence Nationale de la Recherche (LIPOB and OBELIP projects), Région Midi-Pyrénées, Fondation pour la Recherche Médicale, and the Commission of the European Communities (projects DIABAT, HEPADIP, and ADAPT) (to D.L.) and by a grant from Société Francophone du Diabète (to C.M.). We gratefully acknowledge the GenoToul Animal Care, Anexplo, Imaging-TRI, and Quantitative Transcriptomics facilities.

Received: July 2, 2013
Revised: March 10, 2014
Accepted: March 25, 2014
Published: May 1, 2014

REFERENCES

Aoyama, T., Paik, Y.H., and Seki, E. (2010). Toll-like receptor signaling and liver fibrosis. Gastroenterol. Res. Pract. *2010*, 192543.

Biernacka, A., Dobaczewski, M., and Frangogiannis, N.G. (2011). TGF-β signaling in fibrosis. Growth Factors *29*, 196–202.

Bourlier, V., Sengenès, C., Zakaroff-Girard, A., Decaunes, P., Wdziekonski, B., Galitzky, J., Villageois, P., Esteve, D., Chiotasso, P., Dani, C., and Bouloumié, A. (2012). TGFbeta family members are key mediators in the induction of myofibroblast phenotype of human adipose tissue progenitor cells by macrophages. PLoS ONE *7*, e31274.

Campbell, M.T., Hile, K.L., Zhang, H., Asanuma, H., Vanderbrink, B.A., Rink, R.R., and Meldrum, K.K. (2011). Toll-like receptor 4: a novel signaling pathway during renal fibrogenesis. J. Surg. Res. *168*, e61–e69.

Cancello, R., Henegar, C., Viguerie, N., Taleb, S., Poitou, C., Rouault, C., Coupaye, M., Pelloux, V., Hugol, D., Bouillot, J.L., et al. (2005). Reduction of macrophage infiltration and chemoattractant gene expression changes in white adipose tissue of morbidly obese subjects after surgery-induced weight loss. Diabetes *54*, 2277–2286.

Cani, P.D., Amar, J., Iglesias, M.A., Poggi, M., Knauf, C., Bastelica, D., Neyrinck, A.M., Fava, F., Tuohy, K.M., Chabo, C., et al. (2007). Metabolic endotoxemia initiates obesity and insulin resistance. Diabetes *56*, 1761–1772.

Cinti, S., Mitchell, G., Barbatelli, G., Murano, I., Ceresi, E., Faloia, E., Wang, S., Fortier, M., Greenberg, A.S., and Obin, M.S. (2005). Adipocyte death defines

(D) Quantitation of stromavascular fraction cell types in adipose tissue by flow cytometry after 4 weeks of saline or LPS infusion (n = 9 per group).
(E) Adipose tissue macrophage phenotyping by flow cytometry after 4 weeks of saline or LPS infusion (n = 9 per group).
(F) mRNA levels of *Tnf* and fibrosis genes in mouse adipose explants treated with LPS and neutralizing antibody against TGFβ1 (n = 8).
(G) Centroid analysis of five fibrosis pathway genes in mouse adipose explants treated with LPS and neutralizing antibody against TGFβ1 (n = 8).
Values represent mean ± SEM (n = 8 per group). *p < 0.05, **p < 0.01, ***p < 0.001. See also Figure S7.

macrophage localization and function in adipose tissue of obese mice and humans. J. Lipid Res. *46*, 2347–2355.

Divoux, A., Tordjman, J., Lacasa, D., Veyrie, N., Hugol, D., Aissat, A., Basdevant, A., Guerre-Millo, M., Poitou, C., Zucker, J.D., et al. (2010). Fibrosis in human adipose tissue: composition, distribution, and link with lipid metabolism and fat mass loss. Diabetes *59*, 2817–2825.

Divoux, A., Moutel, S., Poitou, C., Lacasa, D., Veyrie, N., Aissat, A., Arock, M., Guerre-Millo, M., and Clément, K. (2012). Mast cells in human adipose tissue: link with morbid obesity, inflammatory status, and diabetes. J. Clin. Endocrinol. Metab. *97*, E1677–E1685.

Gandotra, S., Le Dour, C., Bottomley, W., Cervera, P., Giral, P., Reznik, Y., Charpentier, G., Auclair, M., Delépine, M., Barroso, I., et al. (2011). Perilipin deficiency and autosomal dominant partial lipodystrophy. N. Engl. J. Med. *364*, 740–748.

Henegar, C., Tordjman, J., Achard, V., Lacasa, D., Cremer, I., Guerre-Millo, M., Poitou, C., Basdevant, A., Stich, V., Viguerie, N., et al. (2008). Adipose tissue transcriptomic signature highlights the pathological relevance of extracellular matrix in human obesity. Genome Biol. *9*, R14.

Horng, T., and Hotamisligil, G.S. (2011). Linking the inflammasome to obesity-related disease. Nat. Med. *17*, 164–165.

Li, M., Matsunaga, N., Hazeki, K., Nakamura, K., Takashima, K., Seya, T., Hazeki, O., Kitazaki, T., and Iizawa, Y. (2006). A novel cyclohexene derivative, ethyl (6R)-6-[N-(2-Chloro-4-fluorophenyl)sulfamoyl]cyclohex-1-ene-1-carboxylate (TAK-242), selectively inhibits toll-like receptor 4-mediated cytokine production through suppression of intracellular signaling. Mol. Pharmacol. *69*, 1288–1295.

Keophiphath, M., Achard, V., Henegar, C., Rouault, C., Clément, K., and Lacasa, D. (2009). Macrophage-secreted factors promote a profibrotic phenotype in human preadipocytes. Mol. Endocrinol. *23*, 11–24.

Khan, T., Muise, E.S., Iyengar, P., Wang, Z.V., Chandalia, M., Abate, N., Zhang, B.B., Bonaldo, P., Chua, S., and Scherer, P.E. (2009). Metabolic dysregulation and adipose tissue fibrosis: role of collagen VI. Mol. Cell. Biol. *29*, 1575–1591.

Kim, J.Y., van de Wall, E., Laplante, M., Azzara, A., Trujillo, M.E., Hofmann, S.M., Schraw, T., Durand, J.L., Li, H., Li, G., et al. (2007). Obesity-associated improvements in metabolic profile through expansion of adipose tissue. J. Clin. Invest. *117*, 2621–2637.

Klimcakova, E., Roussel, B., Kovacova, Z., Kovacikova, M., Siklova-Vitkova, M., Combes, M., Hejnova, J., Decaunes, P., Maoret, J.J., Vedral, T., et al. (2011a). Macrophage gene expression is related to obesity and the metabolic syndrome in human subcutaneous fat as well as in visceral fat. Diabetologia *54*, 876–887.

Klimcáková, E., Roussel, B., Márquez-Quiñones, A., Kovácová, Z., Kovácíková, M., Combes, M., Siklová-Vítková, M., Hejnová, J., Srámková, P., Bouloumié, A., et al. (2011b). Worsening of obesity and metabolic status yields similar molecular adaptations in human subcutaneous and visceral adipose tissue: decreased metabolism and increased immune response. J. Clin. Endocrinol. Metab. *96*, E73–E82.

Kusminski, C.M., Holland, W.L., Sun, K., Park, J., Spurgin, S.B., Lin, Y., Askew, G.R., Simcox, J.A., McClain, D.A., Li, C., and Scherer, P.E. (2012). MitoNEET-driven alterations in adipocyte mitochondrial activity reveal a crucial adaptive process that preserves insulin sensitivity in obesity. Nat. Med. *18*, 1539–1549.

Kwon, E.Y., Shin, S.K., Cho, Y.Y., Jung, U.J., Kim, E., Park, T., Park, J.H., Yun, J.W., McGregor, R.A., Park, Y.B., and Choi, M.S. (2012). Time-course microarrays reveal early activation of the immune transcriptome and adipokine dysregulation leads to fibrosis in visceral adipose depots during diet-induced obesity. BMC Genomics *13*, 450.

Lacasa, D., Taleb, S., Keophiphath, M., Miranville, A., and Clement, K. (2007). Macrophage-secreted factors impair human adipogenesis: involvement of proinflammatory state in preadipocytes. Endocrinology *148*, 868–877.

Medina-Gomez, G., Gray, S.L., Yetukuri, L., Shimomura, K., Virtue, S., Campbell, M., Curtis, R.K., Jimenez-Linan, M., Blount, M., Yeo, G.S., et al. (2007). PPAR gamma 2 prevents lipotoxicity by controlling adipose tissue expandability and peripheral lipid metabolism. PLoS Genet. *3*, e64.

Morris, D.L., Singer, K., and Lumeng, C.N. (2011). Adipose tissue macrophages: phenotypic plasticity and diversity in lean and obese states. Curr. Opin. Clin. Nutr. Metab. Care *14*, 341–346.

Nguyen, M.T., Favelyukis, S., Nguyen, A.K., Reichart, D., Scott, P.A., Jenn, A., Liu-Bryan, R., Glass, C.K., Neels, J.G., and Olefsky, J.M. (2007). A subpopulation of macrophages infiltrates hypertrophic adipose tissue and is activated by free fatty acids via Toll-like receptors 2 and 4 and JNK-dependent pathways. J. Biol. Chem. *282*, 35279–35292.

Nguyen, A.T., Mandard, S., Dray, C., Deckert, V., Valet, P., Besnard, P., Drucker, D.J., Lagrost, L., and Grober, J. (2013). Lipopolysaccharides-mediated increase in glucose-stimulated insulin secretion: Involvement of the glucagon-like peptide 1 (GLP1) pathway. Diabetes *63*, 471–482.

Pajvani, U.B., Trujillo, M.E., Combs, T.P., Iyengar, P., Jelicks, L., Roth, K.A., Kitsis, R.N., and Scherer, P.E. (2005). Fat apoptosis through targeted activation of caspase 8: a new mouse model of inducible and reversible lipoatrophy. Nat. Med. *11*, 797–803.

Pardo, A., and Selman, M. (2006). Matrix metalloproteases in aberrant fibrotic tissue remodeling. Proc. Am. Thorac. Soc. *3*, 383–388.

Poggi, M., Bastelica, D., Gual, P., Iglesias, M.A., Gremeaux, T., Knauf, C., Peiretti, F., Verdier, M., Juhan-Vague, I., Tanti, J.F., et al. (2007). C3H/HeJ mice carrying a toll-like receptor 4 mutation are protected against the development of insulin resistance in white adipose tissue in response to a high-fat diet. Diabetologia *50*, 1267–1276.

Rossmeislová, L., Malisová, L., Kracmerová, J., Tencerová, M., Kovácová, Z., Koc, M., Siklová-Vítková, M., Viquerie, N., Langin, D., and Stich, V. (2013). Weight loss improves the adipogenic capacity of human preadipocytes and modulates their secretory profile. Diabetes *62*, 1990–1995.

Saberi, M., Woods, N.B., de Luca, C., Schenk, S., Lu, J.C., Bandyopadhyay, G., Verma, I.M., and Olefsky, J.M. (2009). Hematopoietic cell-specific deletion of toll-like receptor 4 ameliorates hepatic and adipose tissue insulin resistance in high-fat-fed mice. Cell Metab. *10*, 419–429.

Seki, E., De Minicis, S., Osterreicher, C.H., Kluwe, J., Osawa, Y., Brenner, D.A., and Schwabe, R.F. (2007). TLR4 enhances TGF-beta signaling and hepatic fibrosis. Nat. Med. *13*, 1324–1332.

Shi, H., Kokoeva, M.V., Inouye, K., Tzameli, I., Yin, H., and Flier, J.S. (2006). TLR4 links innate immunity and fatty acid-induced insulin resistance. J. Clin. Invest. *116*, 3015–3025.

Spencer, M., Yao-Borengasser, A., Unal, R., Rasouli, N., Gurley, C.M., Zhu, B., Peterson, C.A., and Kern, P.A. (2010). Adipose tissue macrophages in insulin-resistant subjects are associated with collagen VI and fibrosis and demonstrate alternative activation. Am. J. Physiol. Endocrinol. Metab. *299*, E1016–E1027.

Stramer, B.M., Mori, R., and Martin, P. (2007). The inflammation-fibrosis link? A Jekyll and Hyde role for blood cells during wound repair. J. Invest. Dermatol. *127*, 1009–1017.

Strissel, K.J., Stancheva, Z., Miyoshi, H., Perfield, J.W., 2nd, DeFuria, J., Jick, Z., Greenberg, A.S., and Obin, M.S. (2007). Adipocyte death, adipose tissue remodeling, and obesity complications. Diabetes *56*, 2910–2918.

Sun, K., Tordjman, J., Clément, K., and Scherer, P.E. (2013). Fibrosis and adipose tissue dysfunction. Cell Metab. *18*, 470–477.

Tsukumo, D.M., Carvalho-Filho, M.A., Carvalheira, J.B., Prada, P.O., Hirabara, S.M., Schenka, A.A., Araújo, E.P., Vassallo, J., Curi, R., Velloso, L.A., and Saad, M.J. (2007). Loss-of-function mutation in Toll-like receptor 4 prevents diet-induced obesity and insulin resistance. Diabetes *56*, 1986–1998.

Viguerie, N., Montastier, E., Maoret, J.J., Roussel, B., Combes, M., Valle, C., Villa-Vialaneix, N., Iacovoni, J.S., Martinez, J.A., Holst, C., et al. (2012). Determinants of human adipose tissue gene expression: impact of diet, sex, metabolic status, and *cis* genetic regulation. PLoS Genet. *8*, e1002959.

Please cite this article in press as: Vila et al., Immune Cell Toll-like Receptor 4 Mediates the Development of Obesity- and Endotoxemia-Associated Adipose Tissue Fibrosis, Cell Reports (2014), http://dx.doi.org/10.1016/j.celrep.2014.03.062

Virtue, S., and Vidal-Puig, A. (2008). It's not how fat you are, it's what you do with it that counts. PLoS Biol. *6*, e237.

Weisberg, S.P., McCann, D., Desai, M., Rosenbaum, M., Leibel, R.L., and Ferrante, A.W., Jr. (2003). Obesity is associated with macrophage accumulation in adipose tissue. J. Clin. Invest. *112*, 1796–1808.

Wynn, T.A., and Barron, L. (2010). Macrophages: master regulators of inflammation and fibrosis. Semin. Liver Dis. *30*, 245–257.

Xu, H., Barnes, G.T., Yang, Q., Tan, G., Yang, D., Chou, C.J., Sole, J., Nichols, A., Ross, J.S., Tartaglia, L.A., and Chen, H. (2003). Chronic inflammation in fat plays a crucial role in the development of obesity-related insulin resistance. J. Clin. Invest. *112*, 1821–1830.

Zeyda, M., Gollinger, K., Kriehuber, E., Kiefer, F.W., Neuhofer, A., and Stulnig, T.M. (2010). Newly identified adipose tissue macrophage populations in obesity with distinct chemokine and chemokine receptor expression. Int. J. Obes. (Lond.) *34*, 1684–1694.